

## **EFFECT OF ANGULAR POSITION ON POWER GENERATION FROM A PRE-STRESSED PIEZOELECTRIC ELEMENT IN A CAR TIRE**

Solomon Wakolo<sup>1</sup>, John Kihui<sup>2</sup>, Peter Kihato<sup>3</sup>, Kenneth Njoroge<sup>4</sup>

<sup>1,2</sup>Mechanical, JKUAT, Kenya

<sup>3</sup>Electrical, JKUAT, Kenya

<sup>4</sup>Mechanical, UON, Kenya

### **ABSTRACT**

Research on electrical energy harvesting from vibrations, repetitive impacts and bending of structures by means of piezoelectric materials has been done quite extensively in the recent years. With looming shift from fossil fuels to electric cars in the near future, the same knowledge could be applied in automotive car tires to harvest energy that can help power an increasing number of onboard devices as the technology matures. This paper sought to develop a functional car tire model with PZT elements and use it to model the power generated by a single element at different angles and varying forces. This information was then used to develop a predictive model that can be used to estimate the total harvestable piezoelectricity from such a tire. This was achieved by first connecting 12 pieces of 25mm diameter and 0.3mm thick discs together to form an array then binding them together to form a patch of size 115mm by 160mm. This patch was placed in a 185/70R14 tire between the tire carcass and an introduced inner tube. From the series of tests explained in this paper, the power output for each layer of piezoelectric discs was found to be given by  $P_{Tot} = \frac{1.787q^2}{10^6} + \frac{5.276q}{10^4} - \frac{5.025}{10^2}$  Where  $P_{Tot}$  is the power output and q the force at the contact point.

**Keywords:** power harvesting, mechanical vibration, piezoelectric materials, angular position and physical modeling

### **1. INTRODUCTION**

Power harvesting is the process of tapping the waste+ energy surrounding a system and converting it into useful electrical energy[1].

Over the years the possibility of generating power from a rotating tire has been explored quite widely with a desire to efficiently

power the low consumption sensors required in a modern car tire. In this quest, piezoelectric transduction has emerged as the most successful technique of harnessing the vibrational and impact kind of energy experienced at different positions in the rolling tire [2]. There is however still need to explore ways to extract more power from these piezoelectric harvesters in tires with an aim of going a step further and powering some onboard devices. With ample advancement of knowledge in this area, partial powering of the vehicle itself could soon be possible. This is extremely necessary at this particular moment in time because a majority of countries worldwide have set up deadlines for phasing out the gas powered vehicles at around 2040 [3]. As this deadline moves close, need for methods to ensure sufficient electric power is available in the car whenever required increases.

Currently electrical vehicles rely on lithium batteries for their power needs. These batteries come with restricted power when used on their own which limits the range of the vehicle. For this reason, the most viable solution in the long run is likely to be a vehicle equipped with a combination of energy harvesting options in addition to a battery for storing the energy streaming in from different sources. In a few years time we could therefore end up with electric cars having regenerative braking in their design, solar energy harvesters, hydrogen fuel cells, piezoelectric harvesters, Peltier generators as well as a mains recharge unit among

others, ganging up to produce very potent clean power automobiles .

For piezoelectricity to be effective as a candidate in this inevitable future amalgamation of powers sources in automobiles, it is important that the science community has sufficient information on how these harvesters power output behaves under different configuration. Piezoelectric materials are known to exhibit anisotropic characteristics[4]. This means in an application where the orientation of the element in relation to the force source changes like in the case of a rotating car tire, the output is also expected to change at different stages in a given revolution cycle. In this paper, variation in power production with changing angular position of a pre-stressed PZT module in a car tire is looked at.

## **2. LITERATURE REVIEW**

In the simplest terms, when a piezoelectric material is strained mechanically, electric charges collect at the electrodes located on its surface a phenomenon called the direct piezoelectric effect. Optimizing the quantity of this electrical charge generated under different operating conditions is usually the main focus in piezoelectric research. Farnsworth et al noted that for best performance, all piezoelectric energy harvesters require close coupling between the source vibration frequency and its own transduction mechanism [5]. This excitation frequency has to both closely match the

harvester's resonant frequency as well as be steady [6]. These requirements call for frequency tuning of the harvester. The tuning process is however not a straight forward one. As observed by Li et al, the lower the frequency of the host, the more complex it becomes to design the energy harvesting unit[7]. This is majorly because the dimensional and weight constraints limit the use of piezoelectric material due to the relatively high elastic moduli of piezoelectric ceramics used to date. To try and solve this puzzle, Farnsworth et al proposed and tested tying together an evolutionary algorithm (NSGA-II) with a commercial modeling and a simulation tool (COMSOL). Using this arrangement they were able to show that it is possible to optimize the parameterized values of a given shape using soft computing so that its characteristic frequency response matches a target value[5] . Considering the restriction in desirable physical size of a harvester, this still goes on to restrict the source vibration to values above 100Hz[4,6]. In the case of vehicles, such frequencies above 100Hz can be easily achieved from an engine, but maintaining it steadily at 100Hz or any other value when driving a vehicle is big challenge.

To overcome the above source frequency limitations, the harvesting device could be designed to have a wide bandwidth so as to cover all the frequencies expected from the host[4]. Although this ingenious method makes it possible to harvest power from a

range of frequencies, it reduces the peak power harvestable from such a device[4].

Another solution developed is using non resonant generators like those used in bio applications[6]. In particular frequency tuning techniques are not necessary in application involving large direct mechanical impact on the piezoelectric elements[7]. Considering that pre-stressed piezoelectric elements in a rolling tire can be assumed to be exposed to cyclic impact forces, it means frequency tuning in this case is not entirely necessary .This particular finding solves the frequency matching challenge but demands that the performance of the given harvester is evaluated before hand in order to tell its behavior when coupled to the excitation source.

In additional to frequency coupling, design of any piezoelectric harvesting system should also maximize the physical coupling between the kinetic energy source and the transduction mechanism[8]. A pre-stress comes in quite handy at this point, which is why the model proposed in this paper comes with pre-stress.

## **2.1 Piezoelectric Harvester Configurations**

As earlier mentioned, piezoelectric materials are anisotropic, as a result each constant of the piezoelectric material has two subscript notations 'i'and 'j'.

"i" identifies the direction of action (mechanical or electrical) while 'j' identifies

the direction of response. These materials can be generalized for two cases; the first is the stack configuration that operates in the -33 mode and the second is the bender, which operates in the -13 mode[1]. There are also materials that operate in the -15 mode denoting shear as well as materials that operate with different combinations of -13, -33 and -15. The -15 mode materials are said to show the best power performances, the fabrication process they demand is however so complex and expensive that they are not a practical option for power generation application [9].

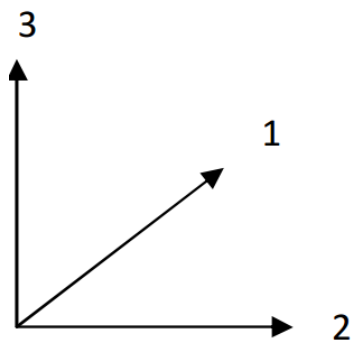


**Figure 1: Denotation of directions**

#### **a. The Bender Configuration**

In bender or  $d_{31}$  operating mode, the piezoelectric layer is polarized in the “3” direction of the piezoelectric and the stress is applied in the “1” direction where the directions are as illustrated in figure 1. In other words the stress is applied perpendicular to the direction of produced electricity.

#### **b. The stack Configurations**

In stack or  $d_{33}$  operating mode, the material is subjected to a stress in the same direction of the produced electric field which is also the poling directions. This  $d_{33}$  elements have been found to develop a greater output voltage than the  $d_{31}$  elements[9]. This property is mainly attributed to their greater voltage coefficient  $g_{33}$ , and larger gap between the electrodes. In these generators, the limiting factor is the length of the piezoelectric material instead of its thickness; hence the gap between electrodes can be made larger than that of  $d_{31}$  devices. Larger gaps however have one limitation, they require greater voltages in order to polarize the piezoelectric material. This increased thickness also compromises the efficiency of poling leading to poor output powers.

Some form of bending is however still experienced in the elements when in the tire. This is because the bender type elements placed in a cantilever have poled directions perpendicular to the planar direction of the piezoelectric layer[7]. The piezoelectric elements in the tire similarly have their poled directions normal to the tire surface, which means the same kind of flexural deflection is also experienced in addition to the cyclic compression of the piezoelectric layer. The tire however has an advantage because unlike a cantilever beam which concentrates the strain around the clamped end[7], the pre-stressed tire uniformly distributes the strain due to bending in the entire disc. In other words whereas bending strain decreases in magnitude at locations

further away from the clamp location in a cantilever, for the pre-stressed tire the strain is kept uniform resulting in better generation. The sign convention assumes that the poling direction is always in the “3” direction. In this particular research the stack configuration that operates in 33 mode is adopted whereby the electric field is applied in the “3” direction and the material is strained in the same poling or “3” direction[1].

## **2.2 Signal Conditioning**

Beeby et al et al observed that the amount of energy generated by piezoelectric devices depends fundamentally upon the kinetic energy available in the application environment and the efficiency of the generator and the power conversion electronics[4]. The Piezoelectric generators give out alternating currents which needs to be rectified for easy accumulation before use. Therefore after proper coupling of the harvester to the excitation source, suitable conditioning is normally selected for efficient harvesting to be achieved. Some of the basic elements used to achieve this conditioning are capacitors for charge storage and diodes for rectification. Umeda et al (1997) established that as the capacitance in conditioning circuit increase, the electrical charge increases as well due to an increased duration of oscillation[1]. Further to this, as voltage increased for each capacitance used in their research, the stored electric charge decreased, and the efficiency increased. Irrinki in his paper points out that

a Series Synchronized Switch Harvesting on Inductor (SSSHI) energy harvesting circuit is usually employed for low frequency applications(less than 10Hz) in order to maximize AC to DC power flow from a piezo-element to a storage capacitor[10]. This circuit comprises of a peak-triggering circuit, inductor, switch, and regulated micro-power step-down converter powered directly from the piezo element and is four times more effective than a full wave rectifier. This research however used a full wave KBP206 rectifier because there are several hardy designs available which could withstand the 30psi pressure

Ottman et al (2002) implemented a DC-DC step down converter with an adaptive control technique to maximize the power flow from a piezoelectric device. This active controller was found to facilitate transfer of over four times the energy transferred with direct charging alone to the connected battery[11]. This was however on condition that the harvester produces more than 10 volts since the controller also consumed power. Kasyap et al (2002) found out in the same year that when a flyback converter is used with a piezoelectric module, a higher peak power efficiency of 20% is achievable [12]. Umeda et al. (1997) did a simulation where the input mechanical energy was translated into an initial electrical energy. During their study they determined that as the capacitance increased the electrical charge increased due to increased duration of oscillation[13].

As noted by Sodano et al in their paper, a piezoelectric power harvesting system would not be a feasible power source for most electronics without provision to accumulate a significant amount of energy[1]. The same team later performed an experiment to compare power storage in a capacitor and a rechargeable battery[11]. They found out that both options could be used but the battery had better capacity hence more steady power output. Suitable circuitry is therefore usually used together with the harvester to store the charge and where possible increase the power that can be drawn at any one time. In this research storage was however avoided in order to track the rapid changes in power production with each impact precisely.

### 2.3 Governing Equations

From dynamic point, a piezoelectric system can be approximated to a damped mass-spring mechanical system as shown in figure 2.

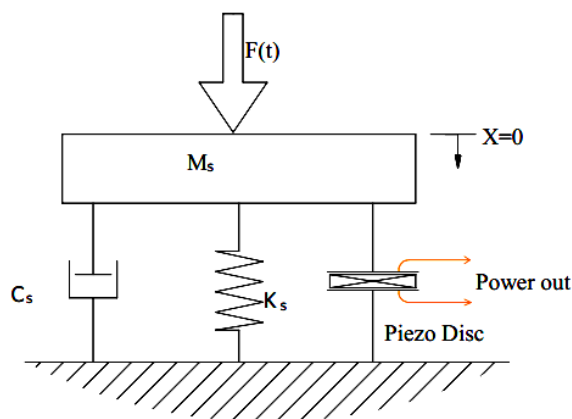


Figure 2: Spring-mass-damper system

The most efficient energy conversion for this system comes from compressing the PZT[14]. The effective power transferred in this way is however minimal, since compression follows the formula

$$\Delta H = \frac{FH}{AE} \tag{1}$$

Where F is the force, H is the unloaded height, A is the area over which the force is applied, and E is the elastic modulus.

It follows that the force at the contact area of the front tires can be estimated by

$$F_{zfl,fr} = \frac{1}{2} m_v \left( \frac{l_r}{l} g - \frac{h}{l} a_x \right) \pm \left( \frac{l_r}{l} g - \frac{h}{l} a_x \right) \frac{h}{e_r g} a_y \tag{2}$$

Where  $a_x$ ,  $a_y$  are the longitudinal and lateral acceleration at the center of gravity in the inertial coordinate system ( $m/s^2$ );  $a_{ym}$  is the measured lateral acceleration ( $m/s^2$ );  $e_f$ ,  $e_r$  are the front and rear vehicle's tracks respectively (m);  $F_{zfl}$   $F_{zfr}$  vertical load on the left front and right front tires (N);  $g$  is the gravitational constant  $9.81 m/s^2$ ;  $h$  is the height of the center of gravity m;  $l_r$  is the distance from the cog to the front and rear axles respectively m;  $m_v$  total mass of the vehicle kg.[15]

Even with these approximation of forces, the load distribution is likely to vary considerably during a journey due to the longitudinal and lateral acceleration of the vehicle [15]. In addition, when a vehicle is cornering the lateral acceleration causes a roll torque which amplifies the load on the

outside tires while diminishing the load on the inside of the vehicle. This therefore means the tire has to be tested for a range of forces above and below the expected force in order to account for the other possible scenarios during driving.

#### 2.4 Selection of Piezoelectric Material

Two very important factors to consider when selecting a piezoelectric material for harvesting purposes are

1. Its electromechanical coupling factor,  $k_{iq}$ , which describes the efficiency with which the material converts mechanical energy into electrical energy

$$k_{iq}^2 = \frac{\text{Electrical Power}}{\text{Mechanical Power}} \quad 3$$

The higher the  $k$  value, the better the material for harvesting purposes

2. Its curie temperature which describes the critical temperature beyond which the material's piezoelectric properties begin to decline. A very high curie temperature is frequently accompanied with a low  $k$  value. As a researcher one therefore has to be aware of the expected operation temperatures in order to select the best material

The piezoelectric materials also come with different physical properties particularly toughness where PZT scores quite poorly in comparison to polymers such as PVDF (polyvinylidene difluoride) or the PZT-

Polymer composites. Based on the above considerations, PZT-5A disks were selected for this study since they have high energy density as well as excellent thermal stability up to  $300^{\circ}\text{C}$ .

As mentioned, even though PZT gives out one of the best energy productions, its major shortcomings as correctly pointed out by Baldisseri et al in their paper, is its fragile nature and tendency to easily fracture [16]. Similarly Makki and Pop-Iliev in their paper revealed that the actual challenge with applying a PZT in a car tire for example 185/65R14, is that the tire requires 3.5 mm of end-to-end deformation for a 40 mm element which is beyond the capacity of many PZT benders available in the market [17]. However other researchers such as Qi et al later showed that it is in fact possible to print PZT ribbons on silicone and end up with a flexible piezoelectric material that doesn't fracture as easily [18]. Rather than pursue the same thought line, in this research the fracture issue was addressed covering the elements in a 4mm thick heat glue (Ethylene-vinyl acetate) jacket. This effectively eliminated fracturing as well as reduced the possible complexity of the assembly that would have resulted from using rubber and PZT.

### 3. METHODOLOGY

Piezoelectric elements of diameter 25mm and a thickness of 0.3mm were soldered into arrays of six connected in parallel as shown in figure 3.

Soldered joints were made in such a way that each element was connected via two different paths to provide an alternative connection in the event of any broken conductors (see appendix A for circuit diagram). Two arrays of six discs each were then connected in series to form a twelve element cluster as shown in figure 3. This developed piezoelectric cluster was connected to a KBP206 rectifier to convert the generated power from AC to DC. Heat glue (Ethylene-vinyl acetate) was generously (approx 2mm thickness on either side) applied on the elements to make a patch as shown in figure 4.

This patch was mounted in a 185/70r14 tire between the car tire carcass and an introduced inner tube as shown in figure 5 and the weight taken

Two introduced nozzles were used as terminals to tap power from inside the tire without leaking the pressurized air in the tire as shown in figure 6.

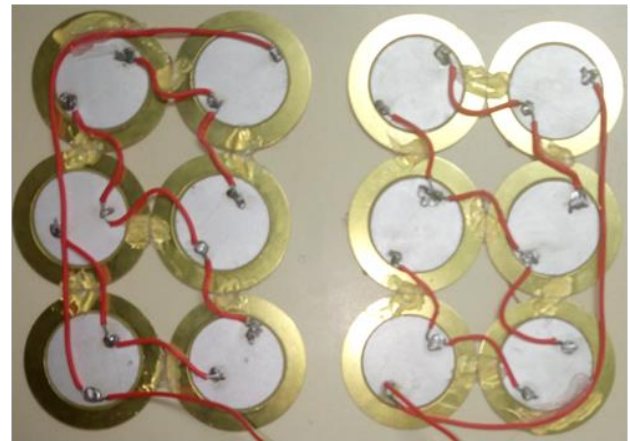


**Figure 3: Assembled piezoelectric discs**



**Figure 4: Assembled Piezoelectric Patch**







Figure 5: Placement of the patch



Figure 6: Complete assembled tire

### Drop Test

The developed tire was taken through a drop test by releasing it from pre-determined heights(2cm, 4cm,6cm, 8cm, 10cm and 12 cm height) to a smooth concrete floor. With each drop, peak electrical outputs (voltage across a 4700 Ohms resistor and current) and deflections were recorded using a video camera. This procedure was repeated three

times for angular positions between 0 degrees and 180 degrees in steps of 10 degrees and the average taken. It is good to note that the choice of using steps of 10 degrees was guided by the capability of the developed rig which could only achieve an accuracy of around  $\pm 2.5^\circ$ .

After finishing the drop tests, the deflection experienced at the contact patch with the different drop heights was measured using the telescopic probe shown in figure 6.



Figure 7: Telescopic probe for measuring deflection at impact

The impact forces were then determined from the relation:

$$F_{imp} = \frac{m \times g \times h}{d} \quad 4$$

Where  $F_{imp}$  is the impact force (N),  $m$  is the mass (Kg),  $g$  is the gravitational field strength (N/Kg),  $h$  is the drop height (m) and  $d$  is the deflection observed on the tire at the time of impact.

The electrical power generated on the other hand was determined from the relation:

$$P = I \times R \quad 5$$

Where P is the power dissipated(Watts), I is the direct current measured(Amps), R is the resistive electric load(Ohms).

The tire was then fixed on a Nissan wingroad DBA-Y12 and tested for around 100Km to establish the toughness of the design(results on power produced when driven will be published in another paper soon to be released).

#### 4. RESULTS

The final weight of the tire after mounting of all the components was found to be 16.25 Kg.

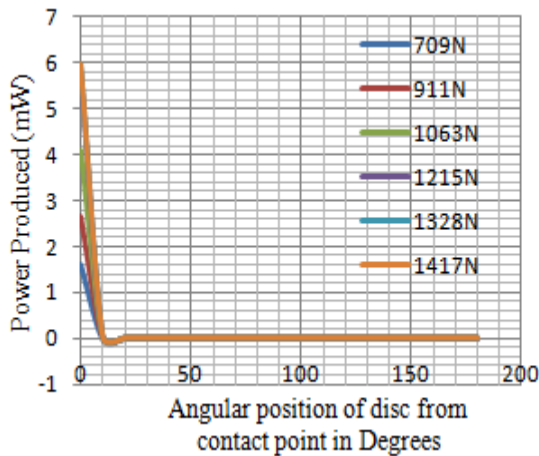


**Figure 8: Graph of Power Output against angular position**

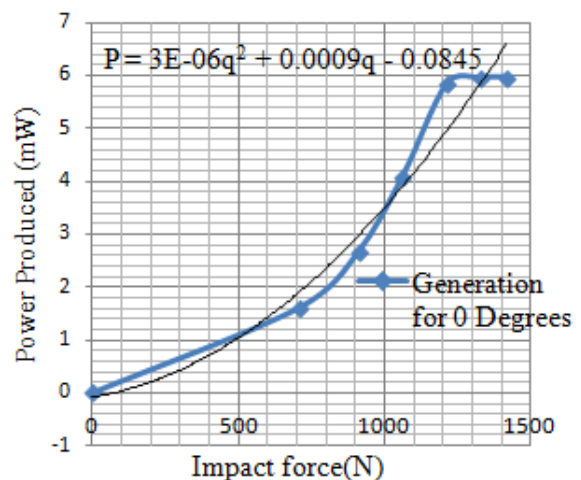
From the recorded peak electrical outputs (voltage and current) and deflections, a graph of power produced against angular

position of PZT discs was plotted as shown in figure 8.

From this plot, the maximum generation of piezoelectric power occurs between 0° and 10°. This region therefore requires the greatest attention when sizing a piezoelectric tire. The same area also experiences the highest variation in generated power with changing impact force. Based on this observation the power generations needs to be evaluated independently for the 0° position, 10 degrees position 20° position and 20°-180° region before coming up with a generalized formula

#### Power Generation by elements at Zero degrees position

The graph in figure 9 shows how power output varies with increasing impact force when the element is positioned directly at the contact patch position.



From this plot the power output from the piezoelectric patch increases steadily with

increasing impact force up to 1200N after which the output remains more or less constant at 6mW. This therefore suggests that with the adopted piezoelectric discs specifications, the patch only needs a force of 1200 N in order to give out its maximum power production. Any additional force above 1200 N should be accompanied with introduction of an additional layer of harvesters.

From the same graph, the power production can be approximated by a polynomial trend-line of degree 2, which is specified as

$$P_o = \frac{3q^2}{10^6} + \frac{9q}{10^4} - \frac{8.45}{10^2} \quad 6$$

Where  $P_o$  is the power output of the patch in mW and  $q$  is the force at the contact patch. This output is however for the entire patch composed of 12 discs. To get the output per disc equation 7 is divided by 12. This action gives

$$p_o = \frac{2.5q^2}{10^7} + \frac{7.5q}{10^5} - \frac{7}{10^3} \quad 7$$

Where  $p_o$  is the power output per PZT disc

This equation is true for  $1 \leq q \leq 1200N$ . It is good to note that since  $q$  includes the weight of the tire under consideration, it can never have a value of zero.

### Power Generation by elements at 10 degrees position

Figure 10 shows a plot of power against impact force when the patch is located 10 degrees from the contact point.

Again at 10 degrees the power output from the piezoelectric patch increases steadily with increasing impact force. This time round the increase however continues all the way to 1400N as opposed to the 1200N witnessed earlier. This could be attributed to the inefficiencies experienced in transmitting the force from the zero degrees position to the new location of the patch. The power output also levels at a very low value of 0.08mW which is only 1.33 percent of the output witnessed when the same element is at 0 degrees position.

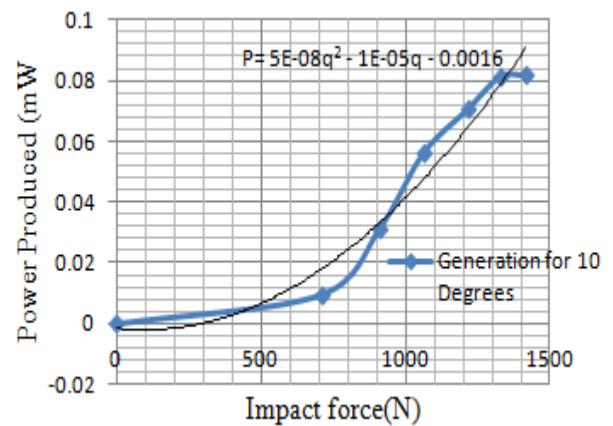


Figure 9: Graph of Power out against Impact force for 10 degrees

This power production can be approximated by a polynomial trend-line of degree 2, which is given by

$$P_{10} = \frac{5q^2}{10^8} - \frac{q}{10^5} - \frac{1.6}{10^3} \quad 8$$

Where  $P_{10}$  is the power output of the patch in mW when positioned 10 degrees from the contact point and  $q$  is the force at the contact

point. To get the output per disc, equation 9 is divided by 12 giving

$$p_{10} = \frac{4.17q^2}{10^9} - \frac{8.33q}{10^7} - \frac{1.33}{10^4} \quad 90$$

Where  $p_{10}$  is the power output per disc

This equation is true for  $1 \leq q \leq 1400N$ .

### Power Generation by elements at 20-180 degrees position

For easier analysis of the data for angles between 20 degrees and 180 degrees, a scatter diagram is plotted as shown in figure 11, and a trend line that best captures the scatter plotted as shown.

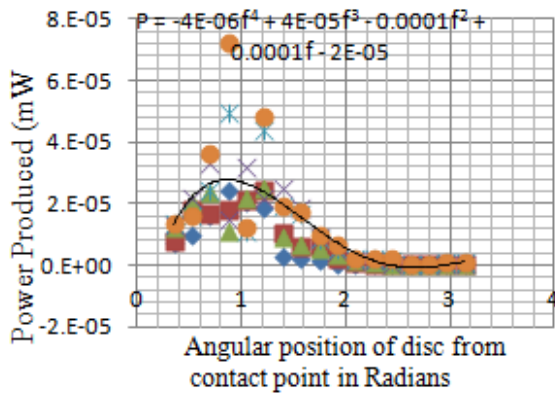


Figure 10: Graph of Power output against angular position

This approach is selected since these values as seen from figure 8, are very close to each other in relation to the outputs observed for the positions 0-10 degrees. From Microsoft excel the above trend line is described by

$$P_{(20-180)} = -\frac{4\phi^4}{10^6} + \frac{4\phi^3}{10^5} - \frac{\phi^2}{10^4} + \frac{\phi}{10^4} - \frac{2}{10^5}$$

It follows that power produced per element will be given by

$$p_{(20-180)} = -\frac{3.33\phi^4}{10^7} + \frac{3.33\phi^3}{10^6} - \frac{8.33\phi^2}{10^6} + \frac{8.33\phi}{10^6} - \frac{1.66}{10^6} \quad 11$$

### Summation of produced power

Taking the following assumptions

1. For the span  $0^\circ-10^\circ$ , the effect of angular changes is approximately linear and hence the power produced by an element mid way can be taken to be the average of the value calculated for that element separately by  $p_0$  and  $p_{10}$
2. For the span  $10^\circ-20^\circ$ , the effect of angular changes is also linear and hence can be taken care of by averaging the value computed separately by  $p_{10}$  and  $p_{20}$
3. For the span  $20^\circ-180^\circ$ , the effect of changing contact force as the vehicle moves is negligible and hence only the influence of angular position needs to be analyzed

It then follows that the total power produced will be given by  $P_{Tot}$

$$P_{Tot} = 2 \times \left( \frac{n_0 p_0}{2} + \frac{1}{2} \left( \sum_{0^\circ}^{10^\circ} p_0 + \sum_{0^\circ}^{10^\circ} p_{10} \right) + n_{10} p_{10} + \frac{1}{2} \left( \sum_{10^\circ}^{20^\circ} p_{10} + \sum_{10^\circ}^{20^\circ} p_{20} \right) + \sum_{20^\circ}^{180^\circ} p_{20-180} \right) \quad 12$$

$$\begin{aligned} \frac{1}{2} P_{Tot} &= \frac{n_{0^{\circ}}}{2} \left( \frac{2.5q^2}{10^7} + \frac{7.5q}{10^5} - \frac{7}{10^3} \right) + \\ &\frac{n_{(0^{\circ}-10^{\circ})}}{2} \left( \left( \frac{2.5q^2}{10^7} + \frac{7.5q}{10^5} - \frac{7}{10^3} \right) + \right. \\ &\left. \left( \frac{4.17q^2}{10^9} - \frac{8.33q}{10^7} - \frac{1.33}{10^4} \right) \right) + n_{10^{\circ}} \left( \frac{4.17q^2}{10^9} - \right. \\ &\left. \frac{8.33q}{10^7} - \frac{1.33}{10^4} \right) + \frac{n_{(10^{\circ}-20^{\circ})}}{2} \left( \left( \frac{4.17q^2}{10^9} - \frac{8.33q}{10^7} - \right. \right. \\ &\left. \left. \frac{1.33}{10^4} \right) + \left( -\frac{3.33\phi_{20^{\circ}}^4}{10^7} + \right. \right. \\ &\left. \left. \frac{3.33\phi_{20^{\circ}}^3}{10^6} - \frac{8.33\phi_{20^{\circ}}^2}{10^6} + \frac{8.33\phi_{20^{\circ}}^1}{10^6} - \frac{1.66}{10^6} \right) \right) + \\ &\sum_{20^{\circ}}^{180^{\circ}} \left( -\frac{3.33\phi^4}{10^7} + \frac{3.33\phi^3}{10^6} - \frac{8.33\phi^2}{10^6} + \right. \\ &\left. \frac{8.33\phi}{10^6} - \frac{1.66}{10^6} \right) \end{aligned} \quad 13$$

$$\begin{aligned} P_{Tot} &= n_{0^{\circ}} \left( \frac{2.5q^2}{10^7} + \frac{7.5q}{10^5} - \frac{7}{10^3} \right) + \\ &n_{(0^{\circ}-10^{\circ})} \left( \frac{2.54q^2}{10^7} + \frac{7.42q}{10^5} - \frac{7.13}{10^3} \right) + \\ &2n_{10^{\circ}} \left( \frac{4.17q^2}{10^9} - \frac{8.33q}{10^7} - \frac{1.33}{10^4} \right) + \\ &n_{(10^{\circ}-20^{\circ})} \left( \frac{4.17q^2}{10^9} - \frac{8.33q}{10^7} - \frac{3.33\phi_{20^{\circ}}^4}{10^7} + \right. \\ &\left. \frac{3.33\phi_{20^{\circ}}^3}{10^6} - \frac{8.33\phi_{20^{\circ}}^2}{10^6} + \frac{8.33\phi_{20^{\circ}}^1}{10^6} - \frac{1.35}{10^4} \right) + \\ &2 \sum_{20^{\circ}}^{180^{\circ}} \left( -\frac{3.33\phi^4}{10^7} + \frac{3.33\phi^3}{10^6} - \frac{8.33\phi^2}{10^6} + \right. \\ &\left. \frac{8.33\phi}{10^6} - \frac{1.66}{10^6} \right) \end{aligned} \quad 14$$

Where  $n_{0^{\circ}}$  is the number of PZT discs at the zero degrees position,  $n_{(0^{\circ}-10^{\circ})}$  is the number of PZT discs between  $0^{\circ}$  and  $10^{\circ}$  position and  $n_{(10^{\circ}-20^{\circ})}$  is the number of PZT discs between  $10^{\circ}$  and  $20^{\circ}$  position.

Taking an example of the 185/70r14 tire used whose specs are

- Diameter = 614.6mm
- Width = 185mm

The inner diameter of the tire, can be computed by subtracting twice the tire thickness from the outside diameter which gives 594.6mm. Since each element has a supporting disc of diameter 35mm and requires an additional spacing of 2.5mm, the maximum number of discs that can be fitted on the face of the tire becomes

$$\frac{185mm}{37.5mm/piece} = 4.93pieces$$

Four pieces per row is however picked since it would be unsafe to force a fifth element along the face of a pressurized tire

Similarly the maximum number of rows that can be placed along the perimeter of the tyre becomes

$$\begin{aligned} &\frac{\text{Internal Tire circumference}}{\text{Space taken by one disc}} \\ &= \frac{\pi \times 594.6mm}{38.5mm/piece} \\ &= \frac{1868}{38.5} pieces = 48.52 \\ &\approx 48rows \end{aligned}$$

Note that in this case 1mm is added to the previous 37.5mm to account for any possible increase or decrease in the diameter during operation. It follows that

$$n_{0^{\circ}} = 1row \times 4pieces = 4pieces$$

1°Corresponds to a distance of  $\frac{1868mm}{360} = 5.189mm$  on the circumference

The remaining segment after placement of the four discs above is given by

$$10^\circ - \left( \frac{18.75mm}{\pi \times 594.6mm} \times 360^\circ \right) = 6.386^\circ$$

This correspond to 33.14mm along the circumference which can only accommodate one row(of 4discs) and spreads to the 10° point though a bigger portion falls in the 0° – 10° region. The following values can therefore be reasonably adopted

$$n_{(0^\circ-10^\circ)} = 3 \text{ pieces and}$$

$$n_{10^\circ}=1\text{piece}$$

It can similarly be shown that

$$n_{10^\circ-20^\circ}=4\text{pieces}$$

$$\varphi_{20^\circ} = 0.349\text{rad}$$

Equation 15 becomes

$$P_{Tot} = 4 \left( \frac{2.5q^2}{10^7} + \frac{7.5q}{10^5} - \frac{7}{10^3} \right) + 3 \left( \frac{2.54q^2}{10^7} + \frac{7.42q}{10^5} - \frac{7.13}{10^3} \right) + 2 \left( \frac{4.17q^2}{10^9} - \frac{8.33q}{10^7} - \frac{1.33}{10^4} \right) + 4 \left( \frac{4.17q^2}{10^9} - \frac{8.33q}{10^7} - \frac{3.33 \times 0.349^4}{10^7} + \frac{3.33 \times 0.349^3}{10^6} - \frac{8.33 \times 0.349^2}{10^6} + \frac{8.33 \times 0.349^3}{10^6} - \frac{1.35}{10^4} \right) + 2 \int_{\pi/9}^{\pi} \left( -\frac{3.33\varphi^4}{10^7} + \frac{3.33\varphi^3}{10^6} - \frac{8.33\varphi^2}{10^6} + \frac{8.33\varphi}{10^6} - \frac{1.66}{10^6} \right) d\varphi \quad 15$$

$$= \left( \frac{1.787q^2}{10^6} + \frac{5.276q}{10^4} - 0.0502 \right) + \left( -\frac{6.66\varphi^5}{5 \times 10^7} + \frac{6.66\varphi^4}{4 \times 10^6} - \frac{1.666\varphi^3}{3 \times 10^5} + \frac{1.666\varphi^2}{2 \times 10^5} - \frac{3.32\varphi}{10^6} + C \right)_{\pi/9}^{\pi} \quad 16$$

$$P_{Tot} = \frac{1.787q^2}{10^6} + \frac{5.276q}{10^4} - \frac{5.025}{10^2} \quad 17$$

Where  $q \leq 1200N$ . Any load above 1200 N per layer should be accompanied with introduction of an additional layer in order to maximize the power production.

It is good to note that the piezoelectric properties change logarithmically with age allowing them to stabilize[16,4]. Manufacturers usually specify the constants of the material after a period of time. This aging process is accelerated by stress applied to the material meaning with continued usage performance is likely to improve, provided the material is not damaged, [4]. This high stress unfortunately also lowers the curie temperature, meaning with the pre-stress, it is important to experimentally evaluate the effect on the generation [4]

#### 4. CONCLUSION

Piezoelectric ceramics particularly PZT have a capacity to produce substantial power that could be harnessed in automobiles to power onboard devices and are among the cheapest piezoelectric materials available. They are however faced with a number of challenges with the main one being their fragile nature which has hindered research in areas involving high forces. In this paper PZT

discs were used to harvest power from a car tire by exposing it to impact forces while protecting them from excessive deflection using contact glue. From the results got, power generation for a 185/70R14 piezoelectric tire with one layer filled with the maximum number of elements per layer (192) will have its output given by

$$P_{Tot} = \frac{1.787q^2}{10^6} + \frac{5.276q}{10^4} - \frac{5.025}{10^2}.$$

For any other type of tire the generalized output is given by equation 15. The results further show that even with the fragile nature of PZT materials, it is still possible to use them in car tires.

### ACKNOWLEDGEMENTS

In this paper we would like to acknowledge JKUAT University for funding this research. We would also like to acknowledge the JKUAT workshop staff in particular automotive workshop and machine shop for their invaluable input during the entire research.

### REFERENCES

- [1] H. A. Sodano, D. J. Inman, and G. Park, "A review of power harvesting from vibration using piezoelectric materials," *Shock Vib. Dig.*, vol. 36, no. 3, pp. 197–205, 2004.
- [2] M. J. Farnsworth, "Design and optimisation of microelectromechanical systems: A review of the state-of-the-art," no. June, 2014.
- [3] M. Schneider, "The Road Ahead for Electric Vehicles," *ICCG Reflect.*, vol. 54, pp. 1–8, 2017.
- [4] S. P. Beeby, R. N. Torah, and M. J. Tudor, "Kinetic Energy Harvesting," in *Energy Harvesting Systems: Principles, Modeling and Applications*, no. January, P. TKazmierski, T. Beeby, Ed. Springer, 2008, pp. 28–29.
- [5] M. Farnsworth, A. Tiwari, and R. Dorey, "Modelling, simulation and optimisation of a piezoelectric energy harvester," *Procedia CIRP*, vol. 22, no. 1, pp. 142–147, 2014.
- [6] P. D. M. P. Miao, B. H. S. E. M. Yeatman, and A. S. H. T. C. Green, "MEMS electrostatic micropower generator for low frequency operation," *Sensors Actuators, A Phys.*, vol. 115, no. 2–3 SPEC. ISS., pp. 523–529, 2004.
- [7] H. Li, C. Tian, and Z. D. Deng, "Energy harvesting from low frequency applications using piezoelectric materials," *Appl. Phys. Rev.*, vol. 1, no. 4, 2014.
- [8] S. P. Beeby, M. J. Tudor, and N. M. White, "Energy harvesting vibration sources for microsystems applications," *Meas. Sci. Technol.*, vol. 17, no. 12, 2006.
- [9] R. Calì, U. B. Rongala, D. Camboni, M. Milazzo, C. Stefanini, G. De Petris, and C. M. Oddo, "Piezoelectric Energy Harvesting Solutions," *Open Access*, vol. 14, no.

- 1424–8220, pp. 4755–4790, 2014.
- [10] P. jayasree Irrinki, “Piezoelectric Energy Harvesting Using Car,” *Int. J. Res. Appl. Sci. Eng. Technol.*, vol. 5, no. X, pp. 616–623, 2017.
- [11] M. B. Yamuna and K. S. Sundar, “Design of Piezoelectric Energy Harvesting and Storage Devices,” *Int. J. Adv. Res. Electr. Electron. Instrum. Eng. (An ISO 3297 2007 Certif. Organ.*, vol. 3, no. 8, pp. 10945–10953, 2014.
- [12] A. Kasyap, J. Lim, D. Johnson, S. Horowitz, T. Nishida, K. Ngo, M. Sheplak, and L. Cattafesta, “Energy reclamation from a vibrating piezoceramic composite beam,” in *Proceedings of 9th International Congress on Sound and Vibration*, 2002, vol. 9, no. 271, pp. 36–43.
- [13] M. Umeda, K. Nakamura, and S. Ueha, “Energy Storage Characteristics of a Piezo-Generator using Impact Induced Vibration,” *Jpn. J. Appl. Phys.*, vol. 36, no. 1, pp. 3146–3151, 1997.
- [14] K. Anil and N. Sreekanth, “Piezoelectric power generation in tires,” *ijeecs*, vol. 2, no. 2/3, pp. 11–16, 2014.
- [15] M. Doumiati, A. Victorino, A. Charara, G. Baffet, and D. Lechner, “An estimation process for vehicle wheel-ground contact normal forces,” in *An estimation process for vehicle wheel-ground contact normal forces*, 2008, pp. 7110–7115.
- [16] G. C. Baldisserri C, Gardini G, “Sharp Silicon/Lead zirconate titanate interfaces by electrophoretic deposition on bare silicon wafers and post deposition sintering,” *Sensors Actuators A Phys.*, vol. 174, no. 0924-4247, pp. 123–132, Feb. 2012.
- [17] N. Makki and R. Pop-Iliev, “Piezoelectric power generation in automotive tires,” in *Smart Materials, Structures & NDT in Aerospace*, 2011, no. November.
- [18] Y. Qi, P. K. Purohit, and M. C. McAlpine, “Enhanced Piezoelectricity and Stretchability in Energy Harvesting Devices Fabricated from Buckled PZT Ribbons,” *Nanoletters*, vol. 11, no. 80311R–80311R–11, p. 1331–1336., 2011.



**APPENDIX**

Appendix A: Circuit Diagram

